

<https://helda.helsinki.fi>

---

## Role of Iodine Recycling on Sea-Salt Aerosols in the Global Marine Boundary Layer

Li, Qinyi

2022-03-28

---

Li, Q, Tham, Y J, Fernandez, R P, He, X-C, Cuevas, C A & Saiz-Lopez, A 2022, 'Role of Iodine Recycling on Sea-Salt Aerosols in the Global Marine Boundary Layer', *Geophysical Research Letters*, vol. 49, no. 6, e2021GL097567. <https://doi.org/10.1029/2021GL097567>

---

<http://hdl.handle.net/10138/354425>

<https://doi.org/10.1029/2021GL097567>

---

cc\_by\_nc\_nd

publishedVersion

---

*Downloaded from Helda, University of Helsinki institutional repository.*

*This is an electronic reprint of the original article.*

*This reprint may differ from the original in pagination and typographic detail.*

*Please cite the original version.*

# Geophysical Research Letters<sup>®</sup>

## RESEARCH LETTER

10.1029/2021GL097567

### Key Points:

- Heterogeneous recycling of iodine on sea-salt aerosol leads to large changes in iodine level and partitioning in the global MBL
- Iodine recycling substantially enhances the production rates of halogen atoms and reduces the levels of oxidants
- Effect of iodine recycling is very sensitive to the uptake efficiency and its range is explored using recently reported coefficients

### Supporting Information:

Supporting Information may be found in the online version of this article.

### Correspondence to:

A. Saiz-Lopez,  
a.saiz@csic.es

### Citation:

Li, Q., Tham, Y. J., Fernandez, R. P., He, X.-C., Cuevas, C. A., & Saiz-Lopez, A. (2022). Role of iodine recycling on sea-salt aerosols in the global marine boundary layer. *Geophysical Research Letters*, 49, e2021GL097567. <https://doi.org/10.1029/2021GL097567>

Received 21 DEC 2021

Accepted 25 FEB 2022

### Author Contributions:

**Conceptualization:** Alfonso Saiz-Lopez

**Formal analysis:** Qinyi Li, Yee Jun Tham, Rafael P. Fernandez, Xu-Cheng He, Carlos A. Cuevas, Alfonso Saiz-Lopez

**Funding acquisition:** Alfonso Saiz-Lopez

**Software:** Qinyi Li, Rafael P. Fernandez, Carlos A. Cuevas, Alfonso Saiz-Lopez

**Validation:** Qinyi Li





**Visualization:** Qinyi Li

**Writing – original draft:** Qinyi Li, Alfonso Saiz-Lopez

© 2022. The Authors.

This is an open access article under the terms of the [Creative Commons Attribution-NonCommercial-NoDerivs License](https://creativecommons.org/licenses/by/4.0/), which permits use and distribution in any medium, provided the original work is properly cited, the use is non-commercial and no modifications or adaptations are made.

## Role of Iodine Recycling on Sea-Salt Aerosols in the Global Marine Boundary Layer

Qinyi Li<sup>1</sup> , Yee Jun Tham<sup>2,3</sup>, Rafael P. Fernandez<sup>4,5</sup> , Xu-Cheng He<sup>3</sup>, Carlos A. Cuevas<sup>1</sup> , and Alfonso Saiz-Lopez<sup>1</sup> 

<sup>1</sup>Department of Atmospheric Chemistry and Climate, Institute of Physical Chemistry Rocasolano, CSIC, Madrid, Spain,

<sup>2</sup>School of Marine Sciences, Sun Yat-Sen University, Zhuhai, China, <sup>3</sup>Institute for Atmospheric and Earth System Research / Physics, Faculty of Science, University of Helsinki, Helsinki, Finland, <sup>4</sup>Institute for Interdisciplinary Science, National Research Council (ICB-CONICET), Mendoza, Argentina, <sup>5</sup>School of Natural Sciences, National University of Cuyo (FCEN-UNCuyo), Mendoza, Argentina

**Abstract** Heterogeneous uptake of hypoiodous acid (HOI), the dominant inorganic iodine species in the marine boundary layer (MBL), on sea-salt aerosol (SSA) to form iodine monobromide and iodine monochloride has been adopted in models with assumed efficiency. Recently, field measurements have reported a much faster rate of this recycling process than previously assumed in models. Here, we conduct global model simulations to quantify the range of effects of iodine recycling within the MBL, using Conventional, Updated, and Upper-limit coefficients. When considering the Updated coefficient, iodine recycling significantly enhances gaseous inorganic iodine abundance (~40%), increases halogen atom production rates (~40% in I, >100% in Br, and ~60% in Cl), and reduces oxidant levels (−7% in O<sub>3</sub>, −2% in OH, and −4% in HO<sub>2</sub>) compared to the simulation without the process. We appeal for further direct measurements of iodine species, laboratory experiments on the controlling factors, and multiscale simulations of iodine heterogeneous recycling.

**Plain Language Summary** The interaction between ocean and atmosphere affects atmospheric chemistry and the climate system. Due to the technical difficulties in direct measurements in the open ocean and coastal environments, the understanding of the marine atmosphere has been heavily dependent on the utilization of multiscale models with limited observational constraints. The development in instrumentation facilitates the direct observation of previously undetected species and unquantified parameters calling for updates of atmospheric models and revisions of the role of relevant processes. Reactive halogen (chlorine, bromine, and iodine) chemistry plays a vital role in controlling the atmospheric composition and oxidation in the marine environment. In particular, iodine chemistry dominates the halogen effects in the marine boundary layer and hypoiodous acid (HOI) is the most abundant iodine species. Recently, field evidence shows that the heterogeneous recycling of iodine is much faster than previously assumed. Here we update a global model with larger coefficients and revisit the role of the HOI heterogeneous processing in marine atmospheric chemistry. These results indicate that the substantial effect of iodine heterogeneous recycling on iodine partitioning, halogen recycling, and oxidant budget may have been underestimated in previous studies and in current models.

## 1. Introduction

Iodine chemistry actively participates in atmospheric chemistry in the marine boundary layer (MBL) and the free troposphere (Saiz-Lopez, Plane et al., 2012). Reactive iodine chemistry is reported to induce significant (10%–20%) reductions in global tropospheric ozone (O<sub>3</sub>) (Saiz-Lopez, Lamarque et al., 2012; Saiz-Lopez et al., 2014; Sherwen, Evans et al., 2016) and to alter the abundance of other oxidants (e.g., OH and HO<sub>2</sub>; Stone et al., 2018). Quantification of the tropospheric impacts of iodine chemistry depends on the understanding of the budget (sources and sinks) of the reactive iodine species.

The main source of atmospheric iodine species arises from the ocean, including the natural emission of very short-lived iodocarbons (CH<sub>3</sub>I, CH<sub>2</sub>I<sub>2</sub>, CH<sub>2</sub>ICl, and CH<sub>2</sub>IBr; Ordóñez et al., 2012) and the O<sub>3</sub>-driven oxidation of aqueous iodide releasing molecular iodine (I<sub>2</sub>) and hypoiodous acid (HOI; Carpenter et al., 2013; MacDonald et al., 2014). These result in elevated levels of iodine species in the MBL, where HOI represents the dominant species (Carpenter et al., 2013; Saiz-Lopez et al., 2014). The subsequent heterogeneous uptake of iodine species, particularly HOI, on sea-salt aerosol (SSA) recycles iodine and activates bromine and chlorine via producing IBR

**Writing – review & editing:** Qinyi Li, Yee Jun Tham, Rafael P. Fernandez, Xu-Cheng He, Carlos A. Cuevas, Alfonso Saiz-Lopez

and ICl which prevents the loss of iodine through deposition to aerosol and ocean surfaces as proposed by Vogt et al. (1996, 1999). Although the reactive uptake coefficient ( $\gamma$ ) for the recycling process in these pioneering studies was not observationally derived, the implementation of SSA-recycling helped to simulate a reasonable amount of iodine species in the MBL. Subsequent modeling studies on iodine chemistry adopted this scheme of iodine recycling on SSA (Badia et al., 2019; Li et al., 2019; Li et al., 2020; Saiz-Lopez, Lamarque et al., 2012; Saiz-Lopez et al., 2014; Sarwar et al., 2015; Sherwen, Evans et al., 2016; Sherwen, Schmidt, et al., 2016) with various uptake coefficients ( $\gamma = 0.01$  to  $0.06$ ) and different production yields (50% IBr and 50% ICl, 100%  $I_2$ , or 15% IBr and 85% ICl), implying the lack of consensus on the HOI heterogeneous uptake efficiency.

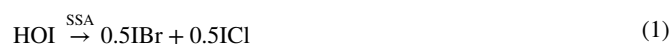
The heterogeneous uptake process of HOI on SSA and its assumed efficiency have not been confirmed in the ambient atmosphere until very recently. Tham et al. (2021) reported the first set of field measurements of HOI, IBr, and ICl at a coastal site in the northern Atlantic (Mace Head) and provided direct evidence of the HOI uptake process on SSA. This work suggests that the HOI uptake proceeds much more rapidly ( $\gamma \geq 0.3$ ) than previously thought, which implies that the role of heterogeneous uptake of HOI on SSA and the subsequent IBr and ICl production (hereafter iodine recycling) in MBL is underestimated in previous studies.

Here, we update a global chemistry-climate model, Community Atmosphere Model with Chemistry (CAM-Chem; Lamarque et al., 2012), to implement the observation-based uptake coefficient range from Tham et al. (2021) for the HOI heterogeneous uptake on SSA. Based on the updated model, we assess the range of impacts of iodine recycling on the abundance and partitioning of reactive iodine species, the production rate of halogen atoms, and the level of key oxidants in the global MBL.

## 2. Methods and Materials

### 2.1. Iodine Chemistry in CAM-Chem

The iodine sources and chemistry in CAM-Chem has been documented in detail elsewhere (Cuevas et al., 2018; Iglesias-Suarez et al., 2020; Ordóñez et al., 2012; Prados-Roman, Cuevas, Fernandez, et al., 2015; Saiz-Lopez et al., 2014). We consider the emission of organic iodine as proposed in Ordóñez et al. (2012) and the inorganic iodine (HOI and  $I_2$ ) emission resulting from atmospheric  $O_3$  deposition onto ocean surface (Carpenter et al., 2013; MacDonald et al., 2014; Prados-Roman, Cuevas, Fernandez, et al., 2015; Figure S1 in Supporting Information S1). CAM-Chem consists of comprehensive iodine chemistry, including photolysis, gas-phase chemistry, and heterogeneous recycling process. Three iodine species (HOI,  $IONO_2$ , and  $INO_2$ ) are taken up onto the SSA to recycle iodine (Equations 1–3), although  $IONO_2$  and  $INO_2$  are generally at low levels in the remote MBL. Please note that although a different ratio of IBr:ICl or different products ( $Cl_2$ ,  $Br_2$ ,  $I_2$ ) following the HOI uptake have been proposed/utilized in previous laboratory/modeling studies (e.g., Enami et al., 2007; Sherwen, Evans et al., 2016; Zhu et al., 2019), in the present study, we follow the direct measurement study of HOI, IBr, and ICl by Tham et al. (2021) and use an equal yield of IBr to ICl as the products following HOI/ $IONO_2$ / $INO_2$  uptake on SSA. Such iodine recycling processes on SSA mostly occur in the lower troposphere where SSA is abundant (Saiz-Lopez et al., 2014). The conventional treatment of HOI in CAM-Chem prior to the present work adopted an uptake coefficient of 0.06. In the present work, we update the HOI uptake coefficient within the range of 0.06 (the conventional value) and 0.9 (the upper-limit proposed in Tham et al., 2021), although most analysis is presented for the simulation with the medium  $\gamma$  (0.3).



### 2.2. Model Simulation Design

The present work follows previous CAM-Chem simulations with specified dynamics (e.g., Fernandez et al., 2014). A horizontal resolution of  $\sim 1^\circ$ , a total of 56 layers from the surface to the stratosphere, and a timestep of 30 min are used. The average results of the lowest seven layers ( $>900$  hPa) represent those in MBL. A previous CAM-Chem

simulation (Veres et al., 2020) was used as the initial condition. The model is run from January 2017 to December 2018 with the first 12 months as the spin-up and the final 12 months for analysis.

We conducted four simulations to isolate the effect of iodine recycling on SSA on atmospheric composition (Table S1 in Supporting Information S1), including the Base ( $\gamma = 0.06$  for the HOI uptake; but no release of IBr and ICl back to the gas phase, i.e., no iodine recycling), Conventional ( $\gamma = 0.06$ ), Updated ( $\gamma = 0.3$ ), and Upper-limit ( $\gamma = 0.9$ ) cases. The Conventional, Updated, and Upper-limit cases considered an equal release of ICl and IBr (50% and 50%, Equation 1). The changes in atmospheric composition (iodine species, other halogen composition, and oxidants) between Base and Updated cases are discussed in detail in Section 3 to represent the effects of iodine heterogeneous recycling. The Conventional and Upper-limit cases are conducted to provide a possible range of iodine recycling effects.

### 2.3. Model Evaluation

The performance of halogen (chlorine, bromine, and iodine) species in CAM-Chem has been intensively evaluated in previous studies (e.g., Ordóñez et al., 2012; Prados-Roman, Cuevas, Hay, et al., 2015; Iglesias-Suarez et al., 2020). In the present work, we also evaluated the CAM-Chem simulated  $O_3$  with coastal observations from the TOAR dataset (Archibald et al., 2020) as depicted in Table S2 and Figure S2 in Supporting Information S1. The evaluation suggests that all simulation cases generally reproduce the magnitude and seasonal variation of the observed  $O_3$  at different coastal sites. The Base case generally over-predicts  $O_3$  in those sites, and the addition of iodine recycling (Conventional, Updated, and Upper-limit cases) generally helps to reduce the prediction bias, with the Updated and Upper-limit cases results closer to the observations. The simulated  $O_3$  deposition velocity (Figure S3 in Supporting Information S1; from  $\sim 0.01$  cm/s to  $\sim 0.1$  cm/s with a global average of 0.046 cm/s over the ocean) is similar to the observation-derived values ranging from 0.006 to 0.15 cm/s (Ganzeveld et al., 2009; Helmig et al., 2012).

A compilation of field measurements of IO is also used to validate the CAM-Chem prediction of IO in the open ocean (Table S3 in Supporting Information S1). The observed IO (daytime average) spanned around the globe covering all seasons from 2006 to 2015 with the largest value (1.7 parts per trillion by volume, pptv) at Cape Verde and the Southern Ocean and the lowest also in the Southern Ocean (0.1 pptv). The predicted daytime (sunlit time) average IO for the year 2018 over these observation sites covers the observational range: in the Base case from 0.15 to 1.61 pptv, Conventional case from 0.26 to 1.75 pptv, Updated case from 0.27 to 1.79 pptv, and Upper-limit case from 0.28 to 1.85 pptv. While all cases captured the observed ranges, please note that the Base case underpredicts IO in most regions and the Updated and Upper-limit cases provide closer predictions of IO compared to the observation in these regions, for example, Cape Verde, West Pacific, Southern Atlantic, Southern Indian Ocean, and Southern Pacific. Our simulated SSA concentrations are also consistent with the observations during the ATom campaigns <https://doi.org/10.3334/ORNLDAAAC/1581>; Figure S4 in Supporting Information S1).

## 3. Results and Discussion

### 3.1. Spatio-Temporal Variation of Iodine Species

Figure 1 shows the annual average spatial distribution of key inorganic iodine species, including  $I_2$ , HOI, IBr, and ICl in the MBL for the Updated case. The inorganic iodine species are mostly confined in the tropical regions particularly along the coast, resulting from the combined effect of atmospheric  $O_3$  level,  $O_3$  deposition rate, radiation intensity, sea-surface temperature, and wind speed (Mahajan et al., 2019, Section 2.1). The distributions of  $I_2$  and HOI mixing ratios are consistent with their emissions (Figure S1 in Supporting Information S1). The distributions of IBr and ICl, formed from the HOI uptake on SSA, are inherently affected by the distribution of HOI and SSA (Figure S5 in Supporting Information S1). Seasonal variations (Figure S6 in Supporting Information S1) show that HOI (similarly, IBr and ICl) in the Indian Ocean peaks in spring (boreal seasons are used throughout the present study), in summer in northern Atlantic, while in the Pacific Ocean and Southern Ocean HOI peaks in autumn and winter, respectively.

Note that the current study represents iodine chemistry for open ocean condition (e.g., Lawler et al., 2014) and the direct emission of  $I_2$  from coastal macroalgae beds (typically in the range of hundreds of meters to a

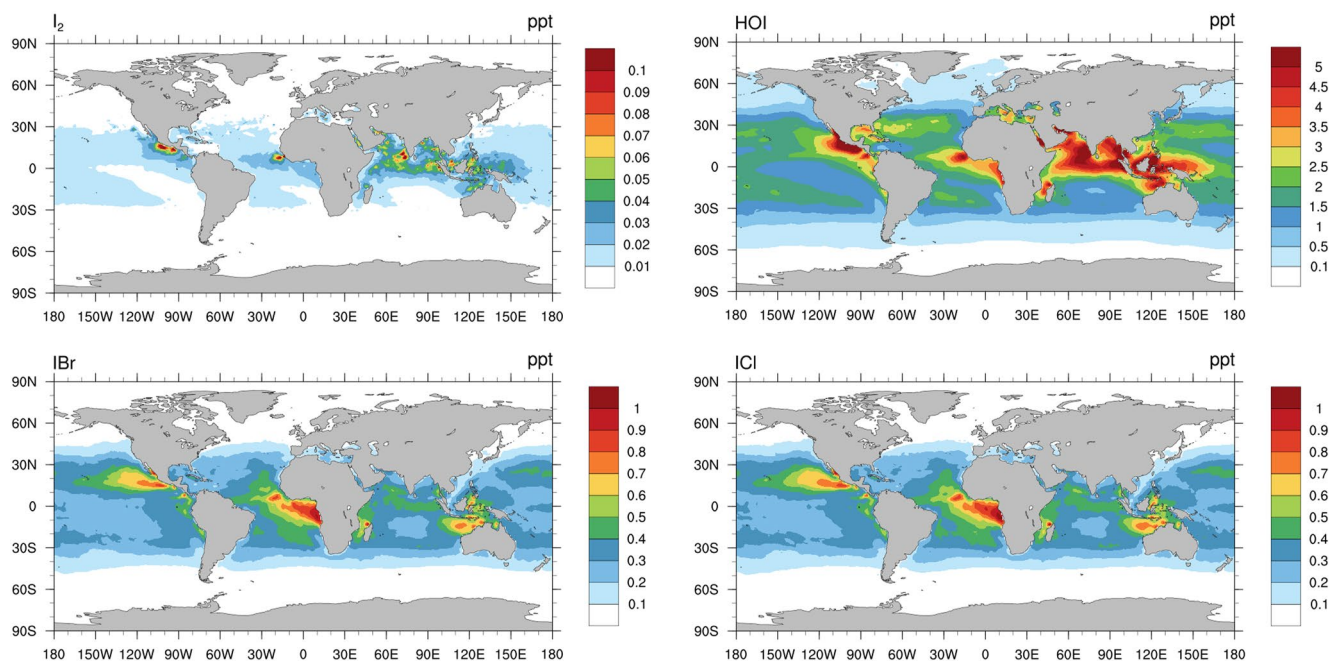


**Figure 1.** Spatial distribution of annual average  $I_2$ , HOI, IBr, and ICl mixing ratios (pptv) in MBL in the Updated case.

few kilometers) is not accounted for in the current setup due to the relatively coarse spatial resolution used in CAM-Chem ( $1^\circ$ ,  $\sim 100$  km in tropics). As a result, large levels of  $I_2$  observed at Mace Head (mainly emitted from macroalgae; Saiz-Lopez & Plane, 2004; Tham et al., 2021) and potentially over other coastal areas with intensive macroalgae emissions, for example, Europe (Mahajan et al., 2011) and Asia (Ghadiryfar et al., 2016), are not well reproduced here.

### 3.2. Iodine Partitioning

Figure 2 depicts the key iodine processes (photolysis, gas-phase reaction, heterogeneous reaction, emission, etc.) in the MBL along with the estimated average mixing ratio of the main inorganic iodine species for the Base (in blue color), Conventional (yellow), Updated (red), and Upper-limit (purple) simulations. The addition of the HOI heterogeneous process on SSA recycles the reactive iodine and substantially increases the level of total inorganic iodine ( $I_y = I + 2I_2 + IO + OIO + HI + HOI + INO + INO_2 + IONO_2 + IBr + ICl + 2I_2O_2 + 2I_2O_3 + 2I_2O_4$ ) from 1.8 pptv (Base) to 2.4 pptv (33% increase; Conventional), 2.5 pptv (38% increase; Updated), and to 2.6 pptv (44% increase; Upper-limit), respectively, in the global MBL. Such results imply that by adopting larger coefficients, that is, faster recycling, HOI heterogeneous uptake leads to higher  $I_y$  level (from 2.4 pptv in Conventional to 2.5 pptv in Updated and 2.6 pptv in Upper-limit cases).

The global- and annual-average levels of IBr (one product of iodine recycling, see Equation 1) are increased from 0.01 (Base) to 0.07 (Conventional), 0.18 (Updated), and 0.27 pptv (Upper-limit). Those of ICl (another product of iodine recycling) increase from 0.01 (Base) to 0.07 (Conventional), 0.19 (Updated), and 0.29 pptv (Upper-limit). The most representative reactive iodine species, IO, is increased from 0.16 (Base) to 0.22 (Conventional), 0.24 (Updated), and 0.25 pptv (Upper-limit). HOI, the dominant inorganic iodine species, is increased from 0.91 pptv in the Base case to 1.14 pptv in the Conventional case; when larger uptake coefficients are adopted, HOI level drops to 1.05 and 0.94 pptv in the Updated and Upper-limit case, respectively, but still higher than that in the Base case. Note that the heterogeneous HOI uptake process is neither a direct sink nor a source of iodine in the atmosphere but instead, the deposited iodine atoms are further stoichiometrically released back into the atmosphere in the form of IBr and ICl, which in turn recycle the iodine atoms through photolysis processes. Finally, oxidation of iodine atoms forms IO which then reacts with  $HO_2$  to form HOI. Therefore, the net effect of the heterogeneous HOI uptake enhances HOI concentration slightly. Without the heterogeneous HOI uptake and the production of gaseous IBr and ICl, HOI (and in turn a significant burden of gas-phase iodine) would primarily be lost to the sea



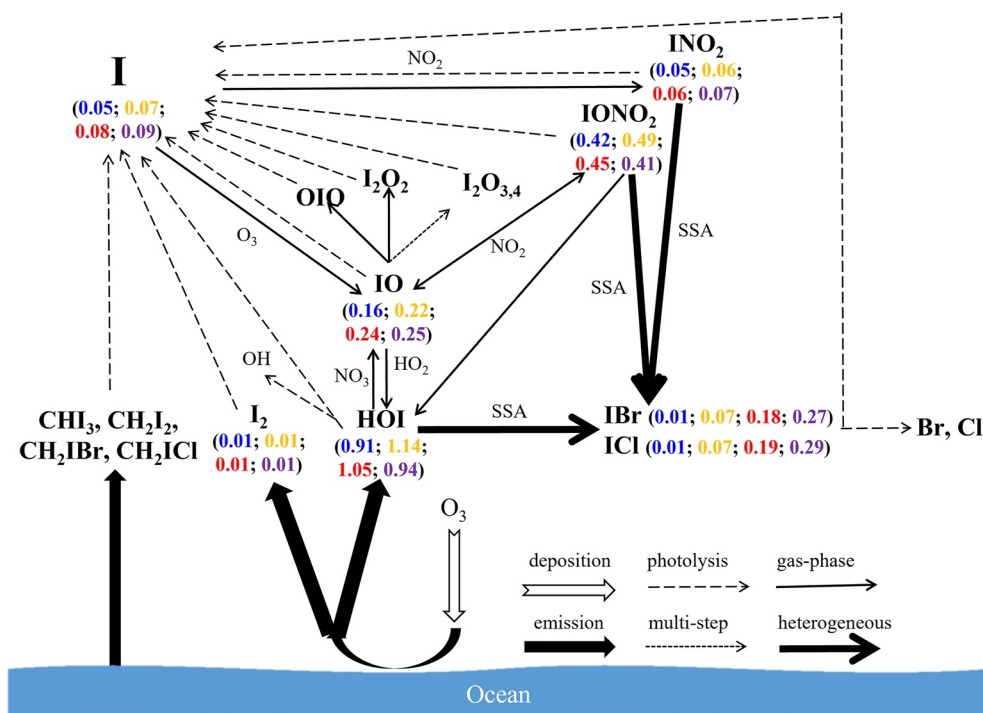


**Figure 2.** Simplified iodine chemistry in the MBL and the simulated mixing ratios (pptv) of the key iodine species in the Base (in blue font), Conventional (yellow), Updated (red), and Upper-limit (purple) cases.

surface or aerosols. Another ocean-emitted species, I<sub>2</sub> remains at a low level in terms of the annual and global MBL average (~0.01 pptv in all cases) because of its fast photolysis and unlike the interhalogens (IBr and ICl), I<sub>2</sub> levels are not affected by the HOI uptake on SSA.

The vertical profile of inorganic iodine species in the lower troposphere for the Base, Conventional, Updated, and Upper-limit cases are depicted in Figure S7 in Supporting Information S1. The abundance of I<sub>y</sub> decreases steadily with height, with HOI being the dominant species in all cases. The portions of IBr and ICl in the Base case are negligible at all altitudes. On the contrary, the sum of IBr and ICl mixing ratios in the other three cases contributes >10% of I<sub>y</sub> throughout the MBL where SSA abundance is noticeable (Figure S5 in Supporting Information S1) and the iodine recycling on SSA occurs, while it decreases to a negligible level in the free troposphere due to their rapid photodissociation and low levels of SSA.

The existing regional and global studies also highlighted the predominant abundance of HOI under various conditions in the troposphere. Previous CAM-Chem studies (with an HOI uptake of 0.06 on SSA to form IBr and ICl; Ordóñez et al., 2012; Saiz-Lopez et al., 2014) simulated the dominant abundance of HOI in the tropical troposphere. Sarwar et al. (2015) added iodine chemistry in the CMAQ model (with no heterogeneous loss of HOI on SSA) and estimated the mean level of HOI to be 2.5 pptv (~15% of total iodine) at the surface in the northern hemisphere while the dominant species was I<sub>2</sub>O<sub>3</sub> due to the omission of I<sub>x</sub>O<sub>y</sub> photolysis. Sherwen, Evans et al. (2016) implemented iodine chemistry in the GEOS-Chem model (with an HOI uptake of 0.01 to form I<sub>2</sub>) and reported the dominant iodine species to be HOI in the global MBL. Li et al. (2019) applied the CMAQ model with HOI uptake (0.01 to form IBr and ICl) and I<sub>x</sub>O<sub>y</sub> photolysis in Europe and reported >50% of HOI contribution to I<sub>y</sub> while the levels of dihalogens and interhalogens were significantly lower within a dominant continental domain over Europe. Badia et al. (2019) incorporated reactive halogen (Cl, Br, and I) sources and chemistry in WRF-Chem including the HOI uptake on SSA ( $\gamma = 0.06$ ) and applied the updated model in the tropical region of western Pacific and their results also showed the dominant abundance of HOI in MBL. Recently, WRF-Chem simulations by Li et al. (2021) predicted >50% I<sub>y</sub> to be HOI (with an uptake of 0.06 to form IBr and ICl) and the dihalogens and interhalogens accounted for ~10% at the surface layer over the West Pacific.

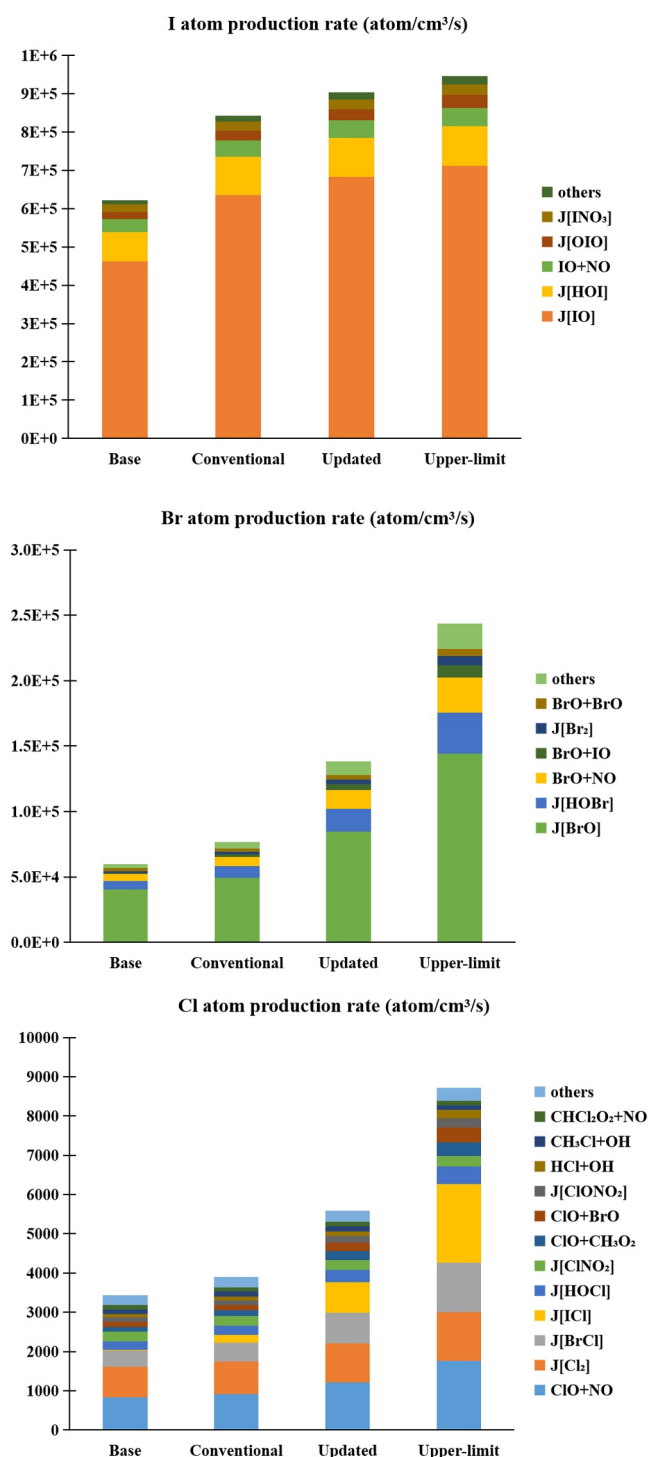


**Figure 3.** Production rate of halogen atoms (I, Br, and Cl) and the contribution of various channels in the MBL in Base, Conventional, Updated, and Upper-limit cases.

### 3.3. Impact of Iodine Recycling on the Production of Halogen Atoms

The simulated production rates of halogen atoms (I, Br, and Cl) in Base, Conventional, Updated, and Upper-limit cases and the contributions from various chemical channels are shown in Figure 3. Note that halogen atom production represents the starting point of halogen-driven atmospheric changes (Figure 2). The consideration of the iodine recycling on SSA substantially enhances the production rates of these three halogen atoms in the MBL. The global- and annual-average production rate of I atom is increased from  $6 \times 10^5$  atom/cm<sup>3</sup>/s (Base) to  $8.4 \times 10^5$  atom/cm<sup>3</sup>/s (Conventional; 35%),  $9 \times 10^5$  atom/cm<sup>3</sup>/s (Updated; 45%), and  $9.5 \times 10^5$  atom/cm<sup>3</sup>/s (Upper-limit; 52%). Similarly, the production rate of Br atom is enhanced from  $6 \times 10^4$  atom/cm<sup>3</sup>/s (Base) to  $7.7 \times 10^4$  atom/cm<sup>3</sup>/s (Conventional; 28%),  $1.4 \times 10^5$  atom/cm<sup>3</sup>/s (Updated; 130%), and  $2.4 \times 10^5$  atom/cm<sup>3</sup>/s (Upper-limit; 300%). The Cl atom production rate is enhanced from 3,500 atom/cm<sup>3</sup>/s (Base) to 3,900 atom/cm<sup>3</sup>/s (Conventional; 13%), 5,500 atom/cm<sup>3</sup>/s (Updated; 60%), and 8,700 atom/cm<sup>3</sup>/s (Upper-limit; 150%).

The enhancement of I atom production is mainly due to IO photolysis (Figure 3). For the Updated case, the level of IO is increased from 0.16 pptv (Base) to 0.24 pptv after the addition of iodine recycling process (Figure 2). Tham et al. (2021) reported that the I atom production rate was increased by 32% due to the iodine recycling at Mace Head and such increase was mainly controlled by IO and OIO photolysis instead of IBr and ICl (~2%). Similarly, the increase in Br atom production ( $\sim 8.0 \times 10^4$  atom/cm<sup>3</sup>/s increase from the Base to Updated) mainly comes from the photolysis of the increased BrO ( $4.4 \times 10^4$  atom/cm<sup>3</sup>/s increase) instead of IBr (700 atom/cm<sup>3</sup>/s increase). The increase of the Cl atom production rate shows a different pattern from I and Br because the photolysis rate of ClO is much slower than IO/OIO and BrO in the MBL. Indeed, the increase in Cl production (2,000 atom/cm<sup>3</sup>/s increase) is driven by the photolysis of ICl (750 atom/cm<sup>3</sup>/s increase), a product of HOI uptake on SSA.

The enhanced recycling of halogen atoms leads to more intensive O<sub>3</sub> destruction (via X + O<sub>3</sub> reaction) and the subsequent decrease in HO<sub>x</sub> production (see Section 3.4). Br and Cl atoms also directly react with non-methane volatile organic compounds (NMVOCs; Atkinson & Aschmann, 1985; Bierbach et al., 1996)—I atom is not reactive to NMVOCs—therefore, the higher production of Br and Cl driven by iodine recycling also implies faster oxidation of VOCs which partially compensates the slower oxidation of VOCs due to the overall decrease of OH levels by halogens. The increase in Br atom production (Figure S8 in Supporting Information S1) could also potentially lead to faster oxidation of atmospheric mercury, a toxic metal (Goodsite et al., 2004; Obrist et al., 2011; Saiz-Lopez et al., 2020). The enhancement in BrO radicals (Figure S8 in Supporting Information S1) due to the faster recycling of iodine on SSA could also result in faster oxidation of dimethyl sulfide, an important sulfur species in the open ocean. The reaction of methane (CH<sub>4</sub>) with OH is the largest chemical loss of CH<sub>4</sub> while that with Cl is the second-largest chemical loss (Kirschke et al., 2013). Therefore, consideration of the iodine recycling on SSA has an influence on the model simulations of the effect of halogens on the burden of CH<sub>4</sub>.

### 3.4. Influence of Iodine Recycling on Atmospheric Oxidants

Figure 4 shows the annual average level of key oxidants, including O<sub>3</sub> (diurnal average), OH (sunlit time average), and HO<sub>2</sub> (sunlit time average), and the effect of iodine recycling on these oxidants (the difference between

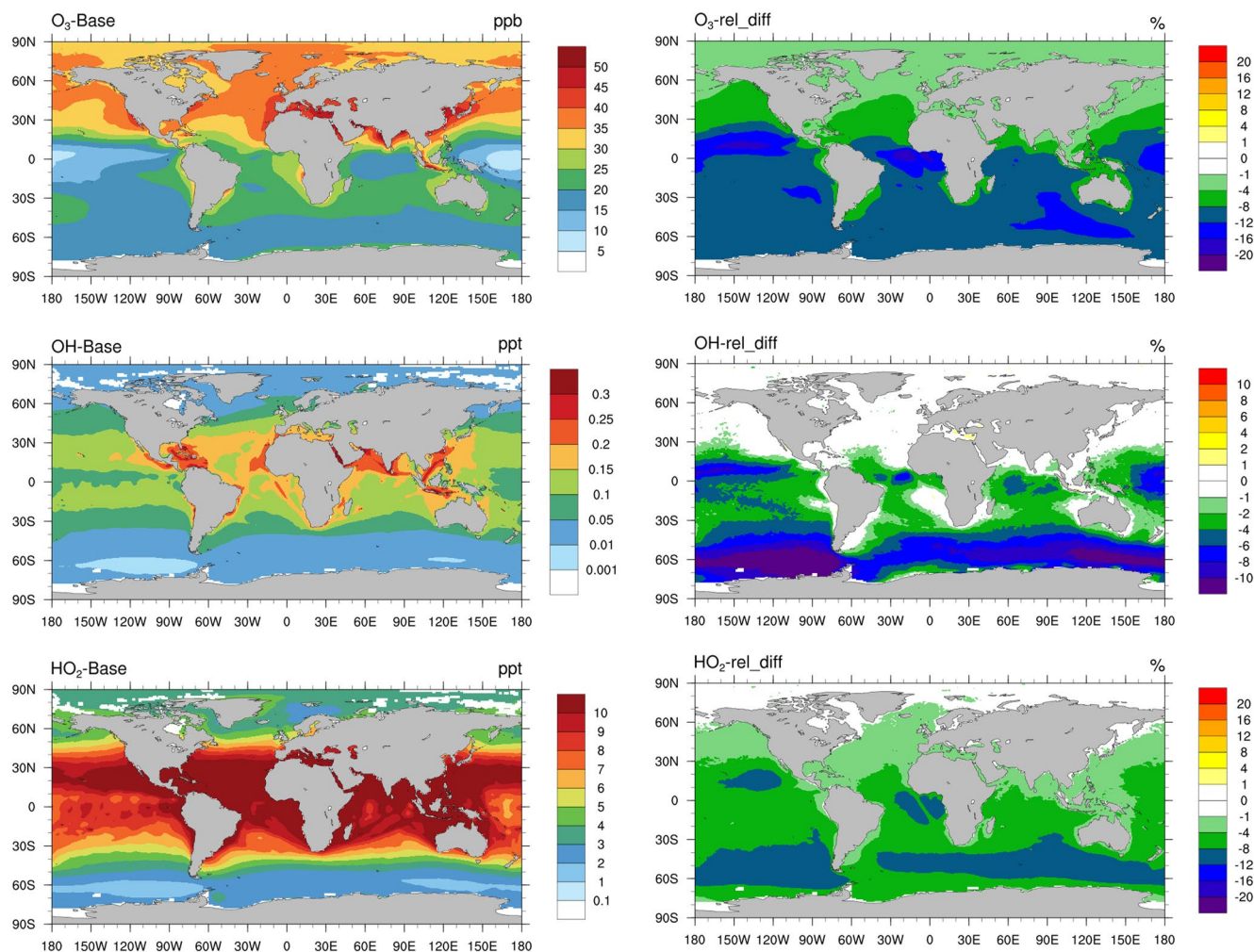


**Figure 4.** Simulated distribution of the annual average of O<sub>3</sub> (ppbv; diurnal average), OH (pptv; sunlit time average), and HO<sub>2</sub> (pptv; sunlit time average) in the Base case in the MBL (left) and the relative change (%) between the Base and Updated cases (right).

Base and Updated case in percentage) in the MBL. The annual average O<sub>3</sub> mixing ratios in the MBL peak in the coastal regions of northern mid-latitudes. The effect of iodine recycling on O<sub>3</sub>, instead, is largest in the tropics and the Southern Ocean and shows a similar spatial distribution as IBr and ICI (Figure 1). The reduction of O<sub>3</sub> from iodine recycling ranges from <1% to ~15% with a global average of ~7%. The OH mixing ratio in the Base case peaks in the tropics and the addition of HOI uptake leads to a reduction in OH in the tropics and the Southern Ocean ranging from <1% to >10%, with an average of 2%. The simulated HO<sub>2</sub> in the Base case shows a similar spatial distribution pattern as OH and the HOI uptake on SSA results in a noticeable decrease in HO<sub>2</sub> levels in MBL with a range of <1% to ~10% and an average of 4%.

The relative changes in oxidants between the Base and Conventional cases and those between Base and Upper-limit cases are shown in Figure S9 in Supporting Information S1 to provide the range of effect of iodine recycling on oxidants. The changes in all three oxidants show a similar spatial pattern but smaller (Conventional) or larger (Upper-limit) changes. The global average change in O<sub>3</sub> in MBL due to iodine recycling is -3.5% (Conventional) to -12% (Upper-limit); similarly, the average change in OH is -1% (Conventional) to -4% (Upper-limit); the average change in HO<sub>2</sub> is -2.5% (Conventional) to -6.6% (Upper-limit). We also calculate the difference in O<sub>3</sub>, OH, and HO<sub>2</sub> between the Conventional and Updated cases and those between the Conventional and the Upper-limit case (Figure S10 in Supporting Information S1). The Updated case results in -3.6%, -1.4%, and -1.8% changes in global average mixing ratios of O<sub>3</sub>, and OH, and HO<sub>2</sub>, respectively, compared to the Conventional case; while the Upper-limit case leads to -9.0%, -3.6%, and -4.2%, respectively. Such results highlight the



potentially much more significant role of HOI and its chemical process in the MBL compared to the existing models.

Global estimates of the iodine recycling effects on oxidants have not been reported. The effect of total reactive iodine on global tropospheric O<sub>3</sub> has been reported to be ~13% to 20% when the HOI uptake coefficient is set to be <0.1 (Iglesias-Suarez et al., 2020; Saiz-Lopez, Lamarque et al., 2012; Saiz-Lopez et al., 2014; Sherwen, Evans, et al., 2016), suggesting that the contribution of iodine heterogeneous recycling using the conventional setting to the total iodine-mediated O<sub>3</sub> loss is ~20%. When a larger coefficient is utilized, a much higher portion (roughly 30%–40%) of iodine-catalyzed O<sub>3</sub> loss could be attributed to HOI uptake on SSA. As a consequence, the total O<sub>3</sub> loss due to iodine in the MBL is expected to be larger than currently simulated by models which demands further investigations.

#### 4. Conclusion

In the present work, we use a global chemistry-climate model, CAM-Chem, to evaluate the potential role of HOI heterogeneous processing in the global MBL. Our numerical experiments show large enhancement effects of the iodine heterogeneous recycling process on the abundance of iodine species and the production rates of bromine and chlorine atoms in the MBL. Such a significant increase in halogen abundance and production leads to a noticeable reduction in the oxidation capacity particularly in the remote oceanic area, for example, the Southern Ocean and central Pacific.

The effects of iodine recycling are very sensitive to the uptake coefficient and larger uptake coefficients (compared to the value used in current models) result in stronger impacts on oxidants, highlighting that the current models underestimate the effect of HOI heterogeneous process on global atmospheric oxidizing capacity. Further direct observations of HOI and other relevant species and parameters are necessary to constrain the efficiency of iodine heterogeneous recycling. Laboratory experiments are also required to identify and quantify the controlling factors of the HOI process and their corresponding efficiency of the different possible production channels (i.e., IBr, ICl, Cl<sub>2</sub>, Br<sub>2</sub>, and I<sub>2</sub>). Simulation studies with various temporal and spatial scales are needed to further comprehend the effect of the iodine heterogeneous recycling process.

#### Data Availability Statement

Data that support the findings of this study can be accessed through Mendeley Data (<https://www.doi.org/10.17632/h3zp6zkc6j.1>). The O<sub>3</sub> observational data at the coastal sites are obtained from the TOAR data set (Archibald et al., 2020; <https://toar-data.org/>).

#### References

- Archibald, A. T., Neu, J. L., Elshorbany, Y. F., Cooper, O. R., Young, P. J., Akiyoshi, H., et al. (2020). Tropospheric ozone assessment report. *Elementa: Science of the Anthropocene*, 8(1), 1–79. <https://doi.org/10.1525/elementa.2020.034>
- Atkinson, R., & Aschmann, S. M. (1985). Kinetics of the gas phase reaction of Cl atoms with a series of organics at 296±2 K and atmospheric pressure. *International Journal of Chemical Kinetics*, 17(1), 33–41. <https://doi.org/10.1002/kin.550170105>
- Badia, A., Reeves, C. E., Baker, A. R., Saiz-Lopez, A., Volkamer, R., Koenig, T. K., et al. (2019). Importance of reactive halogens in the tropical marine atmosphere: A regional modelling study using WRF-chem. *Atmospheric Chemistry and Physics*, 19(5), 3161–3189. <https://doi.org/10.5194/acp-19-3161-2019>
- Bierbach, A., Barnes, I., & Becker, K. H. (1996). Rate coefficients for the gas-phase reactions of bromine radicals with a series of alkenes, dienes, and aromatic hydrocarbons at 298±2 K. *International Journal of Chemical Kinetics*, 28(8), 565–577. [https://doi.org/10.1002/\(sici\)1097-4601\(1996\)28:8<565::aid-kin2>3.0.co;2-t](https://doi.org/10.1002/(sici)1097-4601(1996)28:8<565::aid-kin2>3.0.co;2-t)
- Carpenter, L. J., MacDonald, S. M., Shaw, M. D., Kumar, R., Saunders, R. W., Parthipan, R., et al. (2013). Atmospheric iodine levels influenced by sea surface emissions of inorganic iodine. *Nature Geoscience*, 6(2), 108–111. <https://doi.org/10.1038/ngeo1687>
- Cuevas, C. A., Maffezzoli, N., Corella, J. P., Spolaor, A., Vallelonga, P., Kjaer, H. A., et al. (2018). Rapid increase in atmospheric iodine levels in the North Atlantic since the mid-20th century. *Nature Communications*, 9(1), 1–6. <https://doi.org/10.1038/s41467-018-03756-1>
- Enami, S., Vecitis, C. D., Cheng, J., Hoffmann, M. R., & Colussi, A. J. (2007). Global inorganic source of atmospheric bromine. *The Journal of Physical Chemistry A*, 111(36), 8749–8752. <https://doi.org/10.1021/jp074903r>
- Fernandez, R. P., Salawitch, R. J., Kinnison, D. E., Lamarque, J.-F. F., & Saiz-Lopez, A. (2014). Bromine partitioning in the tropical tropopause layer: Implications for stratospheric injection. *Atmospheric Chemistry and Physics*, 14(24), 13391–13410. <https://doi.org/10.5194/acp-14-13391-2014>
- Ganzeveld, L., Helmig, D., Fairall, C. W., Hare, J., & Pozzer, A. (2009). Atmosphere-ocean ozone exchange: A global modeling study of biogeochemical, atmospheric, and waterside turbulence dependencies. *Global Biogeochemical Cycles*, 23(4).
- Ghadiryfar, M., Rosentrater, K. A., Keyhani, A., & Omid, M. (2016). A review of macroalgae production, with potential applications in biofuels and bioenergy. *Renewable and Sustainable Energy Reviews*, 54, 473–481. <https://doi.org/10.1016/j.rser.2015.10.022>

#### Acknowledgments

This study received funding from the European Research Council Executive Agency under the European Union's Horizon 2020 Research and Innovation Programme (Project ERC-2016-COG 726349 CLIMAHAL). Y.J.T. acknowledges the financial support by the National Natural Science Foundation of China (Grant number: 42175118). R.P.F. would like to thank financial support from ANPCyT (PICT 2019-2187). Computing resources were provided by NCAR's Computational and Information Systems Laboratory (CISL).

- Goodsite, M. E., Plane, J. M. C., & Skov, H. (2004). A theoretical study of the oxidation of Hg<sup>0</sup> to HgBr<sub>2</sub> in the troposphere. *Environmental Science and Technology*, 38(6), 1772–1776. <https://doi.org/10.1021/es034680s>
- Helmig, D., Lang, E. K., Bariteau, L., Boylan, P., Fairall, C. W., Ganzeveld, L., et al. (2012). Atmosphere-ocean ozone fluxes during the TexAQ5 2006, STRATUS 2006, GOMECC 2007, GasEx 2008, and AMMA 2008 cruises. *Journal of Geophysical Research: Atmospheres*, 117(D4).
- Iglesias-Suarez, F., Badia, A., Fernandez, R. P., Cuevas, C. A., Kinnison, D. E., Tilmes, S., et al. (2020). Natural halogens buffer tropospheric ozone in a changing climate. *Nature Climate Change*, 10, 147–154. <https://doi.org/10.1038/s41558-019-0675-6>
- Kirschke, S., Bousquet, P., Ciais, P., Saunois, M., Canadell, J. G., Dlugokencky, E. J., et al. (2013). Three decades of global methane sources and sinks. *Nature Geoscience*, 6(10), 813–823. <https://doi.org/10.1038/ngeo1955>
- Lamarque, J.-F., Emmons, L. K., Hess, P. G., Kinnison, D. E., Tilmes, S., Vitt, F., et al. (2012). CAM-Chem: Description and evaluation of interactive atmospheric chemistry in the community earth system model. *Geoscientific Model Development*, 5(2), 369–411. <https://doi.org/10.5194/gmd-5-369-2012>
- Lawler, M. J., Mahajan, A. S., Saiz-Lopez, A., & Saltzman, E. S. (2014). Observations of I<sub>2</sub> at a remote marine site. *Atmospheric Chemistry and Physics*, 14(5), 2669–2678. <https://doi.org/10.5194/acp-14-2669-2014>
- Li, Q., Badia, A., Fernandez, R. P., Mahajan, A. S., López-Noreña, A. I., Zhang, Y., et al. (2021). Chemical interactions between ship-originated air pollutants and Ocean-emitted halogens. *Journal of Geophysical Research: Atmospheres*, 126(4). <https://doi.org/10.1029/2020JD034175>
- Li, Q., Badia, A., Wang, T., Sarwar, G., Fu, X., Zhang, L., et al. (2020). Potential effect of halogens on atmospheric oxidation and air quality in China. *Journal of Geophysical Research: Atmospheres*, 125, e2019JD032058. <https://doi.org/10.1029/2019JD032058>
- Li, Q., Borge, R., Sarwar, G., de la Paz, D., Gantt, B., Domingo, J., et al. (2019). Impact of halogen chemistry on summertime air quality in coastal and continental Europe: Application of the CMAQ model and implications for regulation. *Atmospheric Chemistry and Physics*, 19(24), 15321–15337. <https://doi.org/10.5194/acp-19-15321-2019>
- MacDonald, S. M., Gómez Martín, J. C., Chance, R., Warriner, S., Saiz-Lopez, A., Carpenter, L. J., & Plane, J. M. C. (2014). A laboratory characterisation of inorganic iodine emissions from the sea surface: Dependence on oceanic variables and parameterisation for global modelling. *Atmospheric Chemistry and Physics*, 14(11), 5841–5852. <https://doi.org/10.5194/acp-14-5841-2014>
- Mahajan, A. S., Sorribas, M., Gómez Martín, J. C., MacDonald, S. M., Gil, M., Plane, J. M. C., & Saiz-Lopez, A. (2011). Concurrent observations of atomic iodine, molecular iodine and ultrafine particles in a coastal environment. *Atmospheric Chemistry and Physics*, 11(6), 2545–2555. <https://doi.org/10.5194/acp-11-2545-2011>
- Mahajan, A. S., Tinel, L., Sarkar, A., Chance, R., Carpenter, L. J., Hulswar, S., et al. (2019). Understanding iodine chemistry over the northern and equatorial Indian Ocean. *Journal of Geophysical Research: Atmospheres*, 124(14), 8104–8118. <https://doi.org/10.1029/2018jd029063>
- Obriet, D., Tas, E., Peleg, M., Matveev, V., Faïn, X., Asaf, D., & Luria, M. (2011). Bromine-induced oxidation of mercury in the mid-latitude atmosphere. *Nature Geoscience*, 4(1), 22–26. <https://doi.org/10.1038/ngeo1018>
- Ordóñez, C., Lamarque, J.-F., Tilmes, S., Kinnison, D. E., Atlas, E. L., Blake, D. R., et al. (2012). Bromine and iodine chemistry in a global chemistry-climate model: Description and evaluation of very short-lived oceanic sources. *Atmospheric Chemistry and Physics*, 12(3), 1423–1447. <https://doi.org/10.5194/acp-12-1423-2012>
- Prados-Roman, C., Cuevas, C. A., Fernandez, R. P., Kinnison, D. E., Lamarque, J.-F., & Saiz-Lopez, A. (2015). A negative feedback between anthropogenic ozone pollution and enhanced ocean emissions of iodine. *Atmospheric Chemistry and Physics*, 15(4), 2215–2224. <https://doi.org/10.5194/acp-15-2215-2015>
- Prados-Roman, C., Cuevas, C. A., Hay, T., Fernandez, R. P., Mahajan, A. S., Royer, S. J., et al. (2015). Iodine oxide in the global marine boundary layer. *Atmospheric Chemistry and Physics*, 15(2), 583–593. <https://doi.org/10.5194/acp-15-583-2015>
- Saiz-Lopez, A., Fernandez, R. P., Ordóñez, C., Kinnison, D. E., Gómez Martín, J. C., Lamarque, J.-F., & Tilmes, S. (2014). Iodine chemistry in the troposphere and its effect on ozone. *Atmospheric Chemistry and Physics*, 14(23), 13119–13143. <https://doi.org/10.5194/acp-14-13119-2014>
- Saiz-Lopez, A., Lamarque, J.-F., Kinnison, D. E., Tilmes, S., Ordóñez, C., Orlando, J. J., et al. (2012). Estimating the climate significance of halogen-driven ozone loss in the tropical marine troposphere. *Atmospheric Chemistry and Physics*, 12(9), 3939–3949. <https://doi.org/10.5194/acp-12-3939-2012>
- Saiz-Lopez, A., & Plane, J. M. C. (2004). Novel iodine chemistry in the marine boundary layer. *Geophysical Research Letters*, 31(4), L04112. <https://doi.org/10.1029/2003GL019215>
- Saiz-Lopez, A., Plane, J. M. C., Baker, A. R., Carpenter, L. J., von Glasow, R., Gómez Martín, J. C., et al. (2012). Atmospheric chemistry of iodine. *Chemical Reviews*, 112(3), 1773–1804. <https://doi.org/10.1021/cr200029u>
- Saiz-Lopez, A., Travnikov, O., Sonke, J. E., Thackray, C. P., Jacob, D. J., Carmona-García, J., et al. (2020). Photochemistry of oxidized Hg(I) and Hg(II) species suggests missing mercury oxidation in the troposphere. *Proceedings of the National Academy of Sciences*, 117(49), 30949–30956. <https://doi.org/10.1073/pnas.1922486117>
- Sarwar, G., Gantt, B., Schwede, D., Foley, K., Mathur, R., & Saiz-Lopez, A. (2015). Impact of enhanced ozone deposition and halogen chemistry on tropospheric ozone over the Northern Hemisphere. *Environmental Science and Technology*, 49(15), 9203–9211. <https://doi.org/10.1021/acs.est.5b01657>
- Sherwen, T., Evans, M. J., Carpenter, L. J., Andrews, S. J., Lidster, R. T., Dix, B., et al. (2016). Iodine's impact on tropospheric oxidants: A global model study in GEOS-chem. *Atmospheric Chemistry and Physics*, 16(2), 1161–1186. <https://doi.org/10.5194/acp-16-1161-2016>
- Sherwen, T., Schmidt, J. A., Evans, M. J., Carpenter, L. J., Großmann, K., Eastham, S. D., et al. (2016). Global impacts of tropospheric halogens (Cl, Br, I) on oxidants and composition in GEOS-chem. *Atmospheric Chemistry and Physics*, 16(18), 12239–12271. <https://doi.org/10.5194/acp-16-12239-2016>
- Stone, D., Sherwen, T., Evans, M. J., Vaughan, S., Ingham, T., Whalley, L. K., et al. (2018). Impacts of bromine and iodine chemistry on tropospheric OH and HO<sub>2</sub>: Comparing observations with box and global model perspectives. *Atmospheric Chemistry and Physics*, 18(5), 3541–3561. <https://doi.org/10.5194/acp-18-3541-2018>
- Tham, Y. J., He, X.-C., Li, Q., Cuevas, C. A., Shen, J., Kalliokoski, J., et al. (2021). Direct field evidence of autocatalytic iodine release from atmospheric aerosol. *Proceedings of the National Academy of Sciences*, 118(4), e2009951118. <https://doi.org/10.1073/pnas.2009951118>
- Veres, P. R., Neuman, J. A., Bertram, T. H., Assaf, E., Wolfe, G. M., Williamson, C. J., et al. (2020). Global airborne sampling reveals a previously unobserved dimethyl sulfide oxidation mechanism in the marine atmosphere. *Proceedings of the National Academy of Sciences*, 117(9), 4505–4510. <https://doi.org/10.1073/pnas.1919344117>
- Vogt, R., Crutzen, P. J., & Sander, R. (1996). A mechanism for halogen release from sea-salt aerosol in the remote marine boundary layer. *Nature*, 383(6598), 327–330. <https://doi.org/10.1038/383327a0>
- Vogt, R., Sander, R., Von Glasow, R., & Crutzen, P. J. (1999). Iodine chemistry and its role in halogen activation and ozone loss in the marine boundary layer: A model study. *Journal of Atmospheric Chemistry*, 32(3), 375–395. <https://doi.org/10.1023/A:1006179901037>
- Zhu, L., Jacob, D. J., Eastham, S. D., Sulprizio, M. P., Wang, X., Sherwen, T., et al. (2019). Effect of sea salt aerosol on tropospheric bromine chemistry. *Atmospheric Chemistry and Physics*, 19(9), 6497–6507. <https://doi.org/10.5194/acp-19-6497-2019>

## References From the Supporting Information

- Dix, B., Baidar, S., Bresch, J. F., Hall, S. R., Schmidt, K. S., Wang, S., & Volkamer, R. (2013). Detection of iodine monoxide in the tropical free troposphere. *Proceedings of the National Academy of Sciences of the United States of America*, *110*(6), 2035–2040. <https://doi.org/10.1073/pnas.1212386110>
- Gómez Martín, J. C., Mahajan, A. S., Hay, T. D., Prados-Román, C., Ordóñez, C., Macdonald, S. M., et al. (2013). Iodine chemistry in the eastern Pacific marine boundary layer. *Journal of Geophysical Research: Atmospheres*, *118*(2), 887–904. <https://doi.org/10.1002/jgrd.50132>
- Großmann, K., Frieb, U., Peters, E., Wittrock, F., Lampel, J., Yilmaz, S., et al. (2013). Iodine monoxide in the western pacific marine boundary layer. *Atmospheric Chemistry and Physics*, *13*(6), 3363–3378. <https://doi.org/10.5194/acp-13-3363-2013>
- Mahajan, A. S., Gómez Martín, J. C., Hay, T. D., Royer, S. J., Yvon-Lewis, S., Liu, Y., et al. (2012). Latitudinal distribution of reactive iodine in the eastern pacific and its link to open ocean sources. *Atmospheric Chemistry and Physics*, *12*(23), 11609–11617. <https://doi.org/10.5194/acp-12-11609-2012>
- Mahajan, A. S., Plane, J. M. C., Oetjen, H., Mendes, L., Saunders, R. W., Saiz-Lopez, A., et al. (2010). Measurement and modelling of tropospheric reactive halogen species over the tropical Atlantic Ocean. *Atmospheric Chemistry and Physics*, *10*(10), 4611–4624. <https://doi.org/10.5194/acp-10-4611-2010>
- Mahajan, A. S., Tinel, L., Hulswar, S., Cuevas, C. A., Wang, S., Ghude, S., et al. (2019). Observations of iodine oxide in the Indian ocean marine boundary layer: A transect from the tropics to the high latitudes. *Atmospheric Environment X*, *1*(January), 100016. <https://doi.org/10.1016/j.aeaoa.2019.100016>
- Read, K. A., Mahajan, A. S., Carpenter, L. J., Evans, M. J., Faria, B. V. E., Heard, D. E., et al. (2008). Extensive halogen-mediated ozone destruction over the tropical Atlantic Ocean. *Nature*, *453*(7199), 1232–1235. <https://doi.org/10.1038/nature07035>